http://dx.doi.org/10.5012/bkcs.2013.34.10.2937

Synthesis of a Novel Near-Infrared Fluorescent Dye: Applications for Fluorescence Imaging in Living Cells and Animals

Tongbin Chen,* Yijun Lai, and Suisheng Huang

*Department of Chemistry, Hanshan Normal University, Chaozhou 521041, P.R. China. *E-mail: chentb@hstc.edu.cn*
Received April 23, 2013, Accepted July 8, 2013

Fluorescence imaging is considered as one of the most powerful techniques for monitoring biomolecule activities in living systems. Near-infrared (NIR) light is advantageous for minimum photodamage, deep tissue penetration, and minimum background autofluorescence interference. Herein, we have developed a new NIR fluorescent dye, namely, RB-1, based on the Rhodamine B scaffold. RB-1 exhibits excellent photophysical properties including large absorption extinction coefficients, high fluorescence quantum yields, and high photostability. In particular, RB-1 displays both absorption and emission in the NIR region of the "biological window" (650-900 nm) for imaging in biological samples. RB-1 shows absorption maximum at 614 nm (500-725 nm) and emission maximum at 712 nm (650-825 nm) in ethanol, which is superior to those of traditional rhodamine B in the selected spectral region. Furthermore, applications of RB-1 for fluorescence imaging in living cells and small animals were investigated using confocal fluorescence microscopy and *in vivo* imaging system with a high signal-to-noise ratio (SNR = 10.1).

Key Words : Near-infrared fluorescent dye, Optical properties, Fluorescence imaging

Introduction

Fluorescence imaging is one of the most powerful techniques for monitoring biomolecule activities in living systems.[1-7] This visualization technology is based on the interactions between light and biological material, and it has been further advanced with the availability of various fluorescent probe molecules.[8] Cellular and tissue imaging at near-infrared (NIR) wavelengths (650-900 nm), the "biological window" for *in vivo* imaging, is advantageous for imaging purposes because the fluorescence emissions in NIR region are not hindered by interfering auto-fluorescence in biological tissues while leaving them with minimum photodamage and deep tissue penetration in the living systems.[9-12] Until now, a large number of fluorescent dyes have been synthesized; however, most of them absorb and emit in the visible range (400-650 nm). In contrast, relatively few fluorescent dyes with both absorption and emission in the NIR region (650-900 nm) are reported, despite their many potential applications in chemical biology. The NIR spectra of these organic molecules are determined by the length of their π-π conjugation structures. Based on this principle, various NIR dyes of different emission wavelengths have been synthesized for use in bioimaging and diagnosis.[13,14]

Rhodamine-based dyes, known for their excellent spectroscopic properties including large molar extinction coefficients, high fluorescence quantum yield, and a high tolerance to photobleaching, have been applied in the study of various biological systems as efficient molecular probes.[15-18] Rhodamine has attracted considerable interest for reliably constructing the "off-on" type fluorochrome probes via the equilibrium between the well-known spirolactam (non-fluorescence) and the ring-opened amide (fluorescence). In particular, the ring-opening process is also accompanied by a vivid color change from colorless to pink, thus enabling naked-eye detection.[19] However, the fluorescence dyes derived from the classic Rhodamine dyes (*e.g.*, Rhodamine 101, Rhodamine 6G, and Rhodamine B) show absorptions and emissions only in the visible region (500-600 nm). This limitation renders them unsuitable for biological imaging in living animals.

Thus, it is highly desirable to develop Rhodamine analogues that absorb and emit in the NIR region. To address this problem, a few NIR Rhodamine analogues have been constructed. For example, Rhodamine 800 is suitable as an NIR-fluorescent probe for biomolecules, however, it is not suitable for designing analyte-responsive sensors, because it has a cyano (CN) functional group instead of a benzoic acid moiety at the 9-position of Rhodamine.[20] Furthermore, Lin *et al.* have synthesized new series of Changsha NIR fluorophores with large absorption extinction coefficients, high fluorescence quantum yields, and high photostability based on Rhodamine analogues.[21] However, based on Rhodamine analogues, there is still scope for the development of more versatile novel NIR dyes for fluorescence imaging.

In this study, we have designed and synthesized a novel NIR dye, namely, RB-1, which is a hybrid of commercially available materials and Rhodamine B analogues, to combine the above optical advantages of Rhodamine B. In particular, RB-1 exhibits both absorption and emission in the NIR region, with an absorption maximum at 614 nm (500-725 nm) and an emission maximum at 712 nm (650-825 nm). Moreover, the applications of RB-1 for fluorescence imaging in living cells and animals were studied using confocal fluorescence microscopy and an *in vivo* bio-imaging system.

Experimental

Materials and Methods. 2-(4-(Diethylamino)-2-hydroxybenzoyl)benzoic acid, *N,N*-styrylbenzenamine, 2-methylpyridine and iodoethane were purchased from J&K Co., Ltd. HEPES and PBS (pH 7.4) was obtained from Sigma-Aldrich Co., Ltd. Toluene, EtOH, CH_3CN, and CH_2Cl_2 were obtained from Guangzhou chemical Co., Ltd. Dry Toluene, CH_3CN, and CH_2Cl_2 were distilled from CaH_2, Methylthiazolyldiphenyl-tetrazolium bromide (MTT) was purchased from Acros Co., Ltd. TLC analysis was performed on silica gel plates and column chromatography was conducted over silica gel (mesh 100-200), both of which were obtained from the Yantai Huanghai Chemicals. All other reagents and solvents were purchased from commercial sources and used without further purification.

Instrumentation. NMR spectra were recorded on Bruker AV400 NMR using TMS as an internal standard. Electrospray ionization mass spectra (ESI-MS) spectra were obtained on a LCMS-2010A system (SHIMADZU) without using the LC part. The electronic absorption spectra were recorded on a GBC Cintra 10 spectrometer. Fluorescence spectra at room temperature were measured on an RF-5301 PC spectrometer. Fourier transform infrared (FT-IR) spectra were measured using a Nicolet Impact-420 spectrophotometer by KBr method. MTT assay was measured with a standard microplate reader (Bio Tek Synergy). Confocal fluorescence imaging was performed by Olympus confocal microscope (IX81, Japan). *In vivo* fluorescence imaging was performed with iBox Scientia 500 imaging system.

Synthesis of Compound 2. To a solution of 2-methylpyridine (30 mmol, 3 g) in dry toluene (10 mL) at room temperature, iodoethane (32 mmol, 5 g) was added. After being refluxed for 24 h, the reaction mixture was cooled and filtered under vacuum. Last, crude product was washed by toluene (10 mL × 3 times) to give compound **2** as a white solid in 75% yield. ^{1}H NMR (400 MHz, $CDCl_3$) δ 9.23 (d, J = 6.1 Hz, 1H), 8.33 (td, J = 7.8, 1.3 Hz, 1H), 7.92 (d, J = 6.6 Hz, 1H), 7.85 (d, J = 8.1 Hz, 1H), 4.93 (d, J = 4.5 Hz, 2H), 4.22 (s, 3H), 1.72 (t, J = 7.2 Hz, 3H). FT-IR: 3130, 2975, 1625, 1580, 1505, 1477, 1456, 1382, 1299, 1170, 1035, 783, 710. MS (ESI) *m/z* calcd for $C_8H_{12}N^+$ (M-I): 122.0. Found: 122.0.

Synthesis of Compound 3. Compound **2** (1 mmol, 1.49 g) and *N,N*-styrylbenzenamine (1 mmol, 1.93 g) were added to 25 mL flask containing 15 mL HAc, and then the reaction mixture was heated to 110 °C and further reacted for 6 h. Last, the crude product was purified by silica gel flash chromatography using CH_2Cl_2/ethanol (20:1) to afford compound **3** in 50% yield. ^{1}H NMR (400 MHz, MeOD) δ 8.51 (d, J = 12.6 Hz, 1H), 8.29 (d, J = 6.4 Hz, 1H), 8.24 (d, J = 8.8 Hz, 1H), 7.95 (t, J = 7.9 Hz, 1H), 7.37 (t, J = 7.9 Hz, 2H), 7.25 (dd, J = 14.3, 7.2 Hz, 3H), 7.09 (t, J = 7.3 Hz, 1H), 6.09 (d, J = 12.6 Hz, 1H), 4.42 (q, J = 7.3 Hz, 2H), 1.53 (t, J = 7.3 Hz, 3H). ^{13}C NMR (100 MHz, MeOD) δ 144.48, 141.91, 140.54, 129.45, 123.44, 121.35, 118.83, 115.84, 90.66, 51.96, 13.26. FT-IR: 3446, 3195, 2975, 1625, 1590, 1552, 1495, 1444, 1293, 1223, 1155, 952, 819, 771, 741, 690, 506. MS (ESI) *m/z* calcd for $C_{15}H_{17}N_2^+$ (M-I): 225.1. Found: 225.2.

Synthesis of Compound 4. Compound 4 was synthesized according to previous literature.[21] Freshly distilled cyclohexanone (13.2 mL, 127.4 mmol) was added dropwise to concentrated H_2SO_4 (120 mL) and cooled down to 0 °C. Then, 2-(4-(diethylamino)-2-hydroxybenzoyl) benzoic acid (64 mmol) was added in portions with vigorous stirring. The reaction mixture was heated at 90 °C for 3 h, cooled down, and poured onto ice (600 g). Perchloric acid (70%, 14 mL) was then added, and the resulting precipitate was filtered off and washed with cold water (500 mL). Compound **4** obtained as a red solid was used for the next step without further purification.

Synthesis of Compound RB-1. Compound **3** (0.21 mmol) and Compound **4** (0.24 mmol) were dissolved in acetic anhydride (6 mL), and the reaction mixture was heated to 80 °C and further stirred for 3 h. Then, water (20 mL) was added to the reaction mixture to quench the reaction. The solvent was removed under reduced pressure to give the crude product, which was purified by silica gel flash chromatography using CH_2Cl_2 to CH_2Cl_2/ethanol (250:1 to 20:3) as eluent to afford RB-1 in 25% yield. ^{1}H NMR (400 MHz, DMSO) δ 8.83 (d, J = 5.6 Hz, 1H), 8.56 (d, J = 13.9

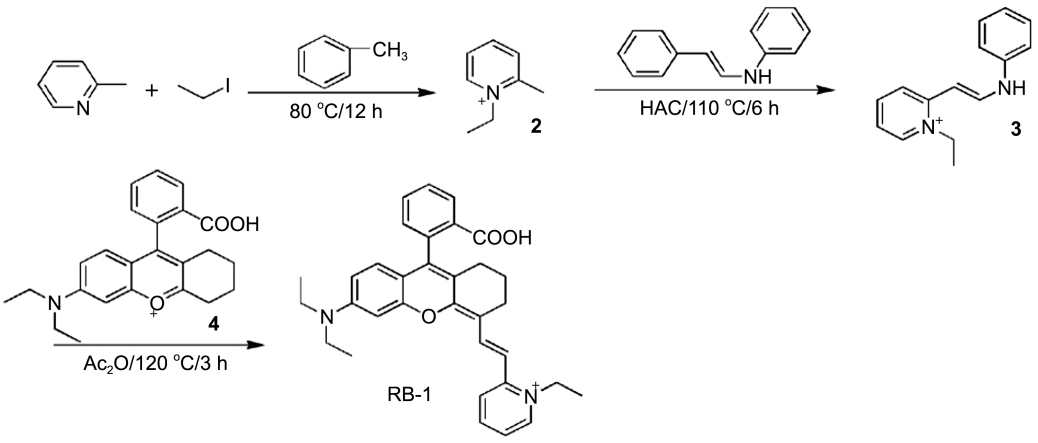

Scheme 1. Synthetic routes of dye RB-1.

Hz, 1H), 8.40 (dd, J = 19.2, 7.6 Hz, 2H), 7.83 (t, J = 6.0 Hz, 1H), 7.63 (dd, J = 17.5, 7.0 Hz, 3H), 7.49 (d, J = 6.9 Hz, 2H), 5.50 (d, J = 13.9 Hz, 1H), 4.55 (d, 2H), 4.28 (d, 2H), 3.36 (d, 2H), 2.19-1.85 (m, 4H), 1.82 (d, 3H), 1.70 (d, 2H), 1.49 (t, J = 7.2 Hz, 3H), 1.12 (t, 6H). FT-IR: 3408, 3041, 2969, 1718, 1624, 1559, 1518, 1490, 1472, 1439, 1353, 1288, 1255, 1222, 1155, 1131, 1070, 854, 816, 767, 705, 619, 537. HR-MS (ESI) *m/z* calcd for $C_{33}H_{35}N_2O_3^+$ (M-ClO_4): 507.2642. Found: 507.2623.

Cell Culture. HeLa (human cervical epitheloid carcinoma) cell lines were provided by the Guangdong Huakai Microbial Sci. &Tech, Co., Ltd. The HeLa cells were grown in culture media (DMEM/F12 supplemented with 10% FBS, 50 unit/mL penicillin, and 50 μg/mL of streptomycin) at 37 °C under a humidified atmosphere containing 5% CO_2 for 24 h. Cells were plated on culture dish and allowed to adhere for 12 h for cell experiments.

Cytotoxicity of RB-1. The *in vitro* cytotoxicity was measured using a standard methyl thiazolyl tetrazolium (MTT) assay. HeLa cells were seeded into 96-well cell culture plate at 1×10^4/well until adherent and then incubated with various concentrations of RB-1 (0, 10, 20, 40 and 60 μmol/L, diluted in DMEM) were then added to the wells. The cells were subsequently incubated for 24 h at 37 °C under 5% CO_2. Thereafter, MTT (5 mg/mL) was added to each well and the plate was incubated for an additional 3 h at 37 °C under 5% CO_2. The quantity of the formazan product formed as measured by the amount of 570 nm absorbance (OD 570) of each well with background subtraction at 690 nm (OD 690) is directly proportional to the number of living cells in the culture. Each experiment was done in triplicate. The relative cell viability (%) related to control wells containing cell culture medium without RB-1was calculated by $[OD]_{expt}/[OD]_{control} \times 100$, where $[OD]_{expt}$ is the absorbance of the test sample and $[OD]_{control}$ is the absorbance of control sample.

Fluorescence Imaging. Confocal fluorescence microscopy imaging of living HeLa cells incubated with the RB-1 was performed on an Olympus confocal fluorescence microscope (IX81, Japan) equipped with a 60 × oil immersion objective lens. For the fluorescence imaging, RB-1 was excited by 633 nm semiconductor lasers and emission output signal was collected by a range 650-750 nm. As a control dye, Rhodamine B (RB) was excited by 543 nm lasers and emission output signal was collected by a range 550-650 nm.

***In vivo* Imaging.** *In vivo* fluorescence imaging was performed with an *in vivo* iBox Scientia 500 imaging system. In this system, adjustable 633 nm lasers were used as the excitation source. Firstly, 50 μL of RB-1 (PBS) was injected intradermally into the subcutaneous tissue. And then, fluorescence imaging *in vivo* was performed under excitation at 633 nm (the power density of 5 mW cm^{-2}) when emission at 668-755 nm was collected with a pass filter (transmission at 650 nm). As a control group, Rhodamine B (RB) was excited by 532 nm laser, collected signal from 550 to 615 nm. Images of fluorescence signal and value of signal to noise ratio (SNR) were analyzed with Vision Works LS Software.

Results and Discussion

Photophysical Properties of RB-1. The electronic extinction and emission spectra of RB-1 in in different solvents (HEPES/ethanol (v/v, 9:1), ethanol, acetonitrile, dichloromethane) at room temperature are shown in Figure 1. RB-1 shows both absorption and emission in the NIR region, with an absorption maximum at 614 nm (500-725 nm) and emission maximum at 712 nm (650-825 nm) in ethanol. The absorption band at maximum at 614 nm is attributed to the 0-0 band of the S0→S1 transition. Moreover, RB-1 also exhibits a very weak and broad absorption band at around 400-450 nm, which can be attributed to the S0→S3 transition.[21] Importantly, RB-1 shows drastic bathochromic absorption and emission peaks in dichloromethane with maximums at 689 and 726 nm, respectively. Thus, the emission of RB-1 covers a significant part of the "biological window" indicating that it could potentially be used as a new NIR dye for biological imaging in living animals. The shape of the absorption spectrum of RB-1 highly resembles that of Rhodamine B, indicating that RB-1 may be an analogue of Rhodamine B.

However, RB-1 has several advantages over Rhodamine B. First, the absorption of RB-1 has a large red shift of about

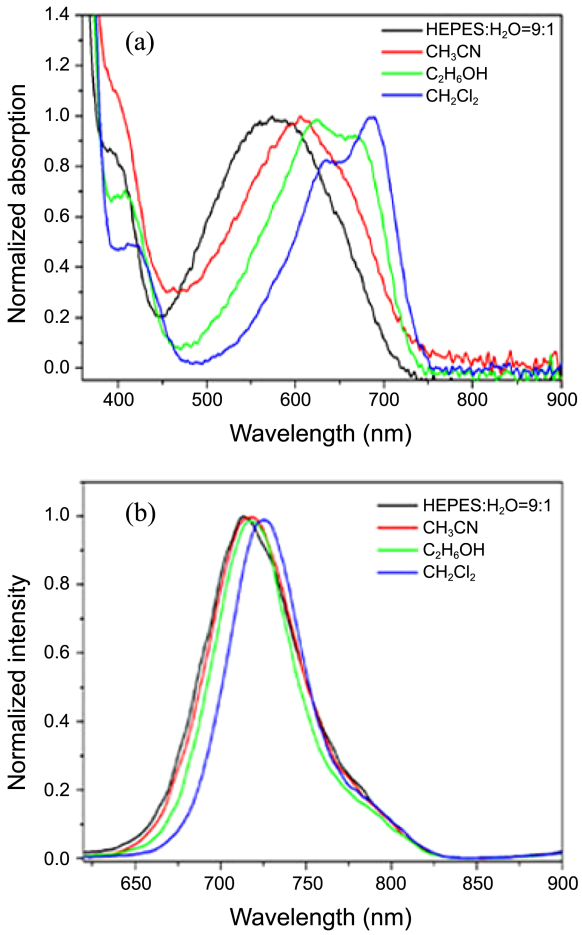

Figure 1. Absorption (a) and fluorescent emission (b) spectra of the RB-1 dispersed in different solvents of HEPES: ethanol = 9:1, ethanol, acetonitrile and dichloromethane.

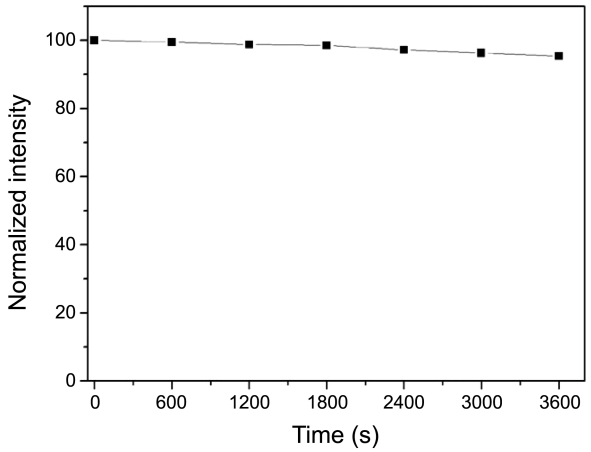

Figure 2. Photostability of RB-1 in ethanol. The samples was continuously irradiated by a xenon lamp (100 W) at the maximal absorption wavelength of RB-1 (614 nm) in ethanol.

60 nm compared to Rhodamine B (λ_{abs} = 552 nm in ethanol). Second, RB-1 has an intense emission peak with a maximum at 712 nm, and extending to 825 nm, that exhibits a drastic bathochromic shift of about 100 nm in emission compared to Rhodamine B (λ_{em} = 610 nm in ethanol). These data suggest that the excitation and emission wavelengths in the RB-1 dye covered the NIR "biological window" for bioimaging.

It is very important to evaluate the photostability of fluorescent dyes intended for extended bioimaging. Therefore, the photostability of RB-1 in ethanol solution was measured under continuous irradiation with a Xe lamp (100 W) at the maximum absorption wavelength of RB-1 (614 nm). The results demonstrate that > 95% of the initial fluorescence intensity was retained after 1 h irradiation (Figure 2), indicating that RB-1 dye has sufficient photostability that is required for potential biological imaging applications.

Cell Fluorescence Imaging. To evaluate the utility of RB-1 dye for bioimaging applications, fluorescence imaging experiment in cells were studied. For tumor cell imaging, HeLa (human cervical epitheloid carcinoma) cells were incubated with RB-1, and observed under an NIR-filtered confocal fluorescence microscope. HeLa cells stained with a 5 μM solution of RB-1 in DMSO/PBS buffer (v/v, 1:99) for 5 min showed clear NIR fluorescence (650-750 nm) in the cytoplasmic regions, confirming that RB-1 is cell-permeable (Figure 3(a), 3(b), 3(c)). The overlay of bright-field and fluorescence images (Figure 3(c)) showed that the fluorescence signal became localized in the intracellular region, which was further confirmed by Z-scan confocal microscopy (Figure S1). The wavelength scan image of living HeLa cells stained with RB-1 was also simultaneously obtained under the same experimental conditions (Figure S2). These results also suggested that the dye is cell-permeable, and suitable for efficient fluorescent imaging in living cells.

To estimate the difference in fluorescent cell imaging between a novel RB-1 and a traditional Rhodamine B (RB) dye, the signals arising from single living cells stained with

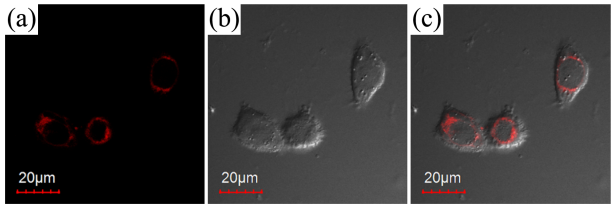

Figure 3. Confocal fluorescence (a), bright-field transmission (b), and overlay (c) images of living HeLa cells incubated with RB-1 (5 μmol/L) for 15 min at 37 °C (λ_{ex} = 633 nm). NIR channel: 650-750 nm.

RB-1 and RB were studied. As shown in Figure S3, the fluorescent intensity profile of RB-1 (maximum intensity ~2010 counts) is obviously stronger than that of RB (maximum intensity ~1620 counts). Therefore, it was concluded that RB-1 dye has a better depth profile for cells than RB.

***In vivo* Fluorescence Imaging of Deep Animal Tissues.** For *in vivo* imaging studies, 50 μL (20 μmol/L) of RB-1 was subcutaneously injected to the side of a live mouse. The *in vivo* fluorescence imaging was performed under excitation at 633 nm (the power density = 5 mW cm^{-2}) from adjustable 633 nm lasers. The signal intensity was clearly observed between the RB-1 location and the bio-background in an NIR imaging system equipped with an NIR emission filter (668-755 nm) (Figure 4(a), 4(b), 4(c)). Moreover, the analysis of the fluorescence signal showed a sensitive imaging performance with a high signal-to-noise ratio (SNR = 10.1) between the RB-1 location and the background through the analysis software, stating that the *in vivo* signal from the RB-1 location is ten times more intense compared to the bio-background.

In order to compare the deep penetration *in vivo* imaging of a novel fluorescent dye RB-1, the traditional dye Rhodamine B (RB) was selected as the control dye. As shown in Figure S4(a), distinct signals were only obtained from the location containing RB-1, rather than RB, which clearly indicate that RB-1 had a deeper penetration compared to RB under excitation at 633 nm light, and the signal-to-noise ratio (SNR) > 9. Further, to test the penetration of RB, 532 nm light was selected as the excitation wavelength, and the *in vivo* fluorescence images of the RB were obtained. In the Figure S4(b), the signals were detected from the location containing RB, and a SNR of ~5 was obtained, which was less than that obtained for RB-1. In summary, the *in vivo*

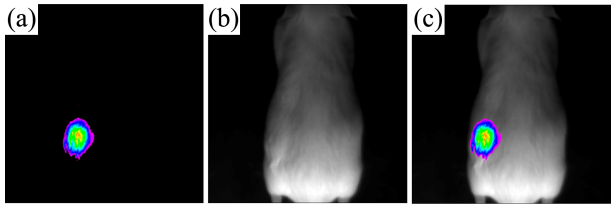

Figure 4. *In vivo* NIR fluorescence imaging (a: NIR fluorescence, b: optical brightfield, c: overlaid of optical brightfield and pseudo-colored NIR fluorescence) of a live mouse subcutaneously injected with 50 μL of RB-1 (20 μmol/L in PBS). λ_{ex} = 633 nm (the power density of 5 mW cm^{-2}), collected NIR signal from 668 to 755 nm.

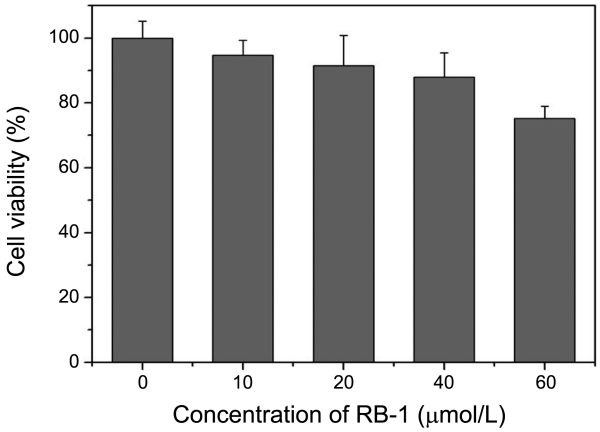

Figure 5. Viability estimated by MTT proliferation test of HeLa cells incubation of RB-1 at 37 °C for 24 h. HeLa cells were cultured in the presence of 10-60 μmol/L RB-1.

fluorescence imaging of small animal using RB-1 with both high-contrast and red light excitation could be achieved. RB-1 may find use in dermal or sub-dermal imaging of pathologic conditions such as melanomas and warts, as well as for the mucosal and sub-mucosal pathologies.

Cytotoxicity of RB-1. The HeLa cell lines were treated with different concentrations of RB-1 to determine the cytotoxicity, and the toxicity data are shown in Figure 5. The viability of non-treated cells is assumed to be 100%. At a 10 μmol/L RB-1 concentration, incubation of the cells for 24 h did not change the cell viability, and less than 5% of the HeLa cells died. When the RB-1 concentration was increased to 40 μmol/L, the cell viability remained above 80%. However, no sub-cellular apoptotic changes or significant cell death was observed in the cells after incubation with working concentrations for imaging (5 μmol/L for cell imaging and 20 μmol/L for the *in vivo* small animal imaging), and the cell viability of RB-1 for HeLa is still kept above 95%, even with the incubation time of 24 h. In general, RB-1 exhibits low cytotoxicity when used in a certain range of concentrations and within limited time periods of incubation.

Conclusion

In summary, we have developed a NIR dye, namely, RB-1, by employing a scaffold of Rhodamine analogues. The proposed RB-1 dye can be efficiently synthesized. Importantly, RB-1 is found to be superior than the reported traditional Rhodamine B dye both with respect to absorption and emission, and having an absorption maximum at 614 nm (500-725 nm) and emission maximum at 712 nm (650-825 nm). Furthermore, fluorescence imaging of living cells and *in vivo* small animals with RB-1 could be achieved, and it displayed high sensitivity and photo-stability. RB-1 could be employed as a molecular tool for biological detection and imaging. Future effort should be focused on further developing more efficient fluorescent sensors in the NIR range based on the studies with RB-1.

Acknowledgments. This work was supported by the Funds of Science and Technology Department of Guangdong Province (2008B080701017) and Funds of Hanshan Normal University (LY201305). And the publication cost of this paper was supported by the Korean Chemical Society.

References

1. Stchur, P.; Cleveland, D.; Zhou, J.; Michel, R. G. *Appl. Spectrosc. Rev.* **2002**, *37*, 383.
2. Loudet, A.; Burgess, K. *Chem. Rev.* **2007**, *107*, 4891.
3. Gonçalves, M. S. T. *Chem. Rev.* **2008**, *109*, 190.
4. Baumes, J. M.; Gassensmith, J. J.; Giblin, J.; Lee, J.-J.; White, A. G.; Culligan, W. J.; Leevy, W. M.; Kuno, M.; Smith, B. D. *Nat. Chem.* **2010**, *2*, 1025.
5. Ueno, T.; Nagano, T. *Nat. Methods* **2011**, *8*, 642.
6. Schaafsma, B. E.; Mieog, J. S. D.; Hutteman, M.; van der Vorst, J. R.; Kuppen, P. J. K.; Löwik, C. W. G. M.; Frangioni, J. V.; van de Velde, C. J. H.; Vahrmeijer, A. L. *J. Surg. Oncol.* **2011**, *104*, 323.
7. Nothdurft, R.; Sarder, P.; Bloch, S.; Culver, J.; Achilefu, S. *J. Microsc.* **2012**, *247* , 202.
8. Kiyose, K.; Aizawa, S.; Sasaki, E.; Kojima, H.; Hanaoka, K.; Terai, T.; Urano, Y.; Nagano, T. *Chem.-Eur. J.* **2009**, *15*, 9191.
9. Fabian, J.; Nakazumi, H.; Matsuoka, M. *Chem. Rev.* **1992**, *92*, 1197.
10. Kobayashi, H.; Longmire, M. R.; Ogawa, M.; Choyke, P. L. *Chem. Soc. Rev.* **2011**, *40*, 4626.
11. Ntziachristos, V.; Bremer, C.; Weissleder, R. *Eur. Radiol.* **2003**, *13*, 195.
12. Jensen, E. C. *Anat. Rec.* **2012**, *295*, 2031.
13. Sevick-Muraca, E. M.; Houston, J. P.; Gurfinkel, M. *Curr. Opin. Chem. Biol.* **2002**, *6*, 642.
14. Yuan, A.; Wu, J.; Tang, X.; Zhao, L.; Xu, F.; Hu, Y. *J. Pharm. Sci.* **2013**, *102*, 6.
15. Zheng, H.; Qian, Z. H.; Xu, L.; Yuan, F. F.; Lan, L. D.; Xu, J. G. *Org. Lett.* **2006**, *8*, 859.
16. Beija, M.; Afonso, C. A. M.; Martinho, J. M. G. *Chem. Soc. Rev.* **2009**, *38*, 2410.
17. Jun, M. E.; Ahn, K. H. *Org. Lett.* **2010**, *12*, 2790.
18. Shi, W.; Sun, S.; Li, X.; Ma, H. *Inorg. Chem.* **2009**, *49*, 1206.
19. Yang, Y. M.; Zhao, Q.; Feng, W.; Li, F. Y. *Chem. Rev.* **2013**, *113*, 192.
20. Abugo, O. O.; Nair, R.; Lakowicz, J. R. *Analy. Biochem.* **2000**, *279*, 142.
21. Yuan, L.; Lin, W.; Yang, Y.; Chen, H. *J. Am. Chem. Soc.* **2011**, *134*, 1200.